A Prototype Two-Decade Fully-Coupled Fine-Resolution CCSM Simulation

Julie L. McClean[1,2], David C. Bader[3,2], Frank O. Bryan[4], Mathew E. Maltrud[5], John M. Dennis[4], Arthur A. Mirin[2], Philip W. Jones[5], Mariana Vertenstein[4], Detelina P. Ivanova[2], Yoo Yin Kim[1], James S. Boyle[2], Robert L. Jacob[6], Nancy Norton[4], Anthony Craig[4], and Patrick H. Worley[3]

[1]*Scripps Institution of Oceanography, La Jolla, CA 92093*

[2]*Lawrence Livermore National Laboratory, Livermore CA 94551*

[3]*Oak Ridge National Laboratory, Oak Ridge, TN 37831*

[4]*National Center for Atmospheric Research, Boulder, CO 80303*

[5]*Los Alamos National Laboratory, Los Alamos, NM 87545*

[6]*Argonne National Laboratory, Argonne, IL 60439*

Corresponding author address: Dr Julie L. McClean

Climate, Atmospheric Science and Physical Oceanography Division

Scripps Institution of Oceanography, La Jolla, CA 92093-0230.

Email: jmcclean@ucsd.edu

Abstract

A fully coupled global simulation using the Community Climate System Model (CCSM) was configured using grid resolutions of 0.1° for the ocean and ice, and 0.25° for the atmosphere and land, and was run under present-day greenhouse gas conditions for 20 years. Intensified and contracted polar vortices, and too cold sea surface temperatures (SSTs) in the subpolar and mid-latitude Northern Hemisphere were the dominant biases produced by the model. Intense category 4 cyclones formed spontaneously in the tropical North Pacific and the ocean response to one such event shows the realistic formation of a cold SST wake, mixed layer deepening, and warming below the mixed layer. Agulhas eddy pathways are more realistic than in equivalent stand-alone ocean simulations forced with atmospheric reanalysis.

Introduction

Simulating the Earth System realistically under present day conditions, a necessary precursor to climate projection, is a major scientific challenge. The veracity of current-generation simulations is undermined by missing and inadequately represented processes in component models together with feedback errors within and among components (Large and Danabasoglu, 2006). Generally the use of finer resolution in atmospheric global climate models has led to systematic improvements in the fidelity of atmospheric features, particularly those associated with the large-scale dynamical circulation (Hack et al. 2006). Increased resolution in ocean-only simulations has improved the mean state and variability of the simulated ocean circulation, by explicitly resolving most mesoscale (50 to 500 km and 20 and 150 days) fluctuations (McClean et al., 2006).

Here we present results from a two-decade, present-day simulation of a prototype version of the Community Climate System Model version 4 (CCSM4) where a weather-scale resolution atmospheric model is coupled to an eddy-resolving ocean. Others have coupled combinations of high and low-resolution components in the CCSM framework such as Gent et al. (2009) who use 0.5° atmospheric/land and nominal 1° oceanic/ice components. This is the first study with CCSM, to our knowledge, where all components have fine enough horizontal resolution for both the ocean and atmosphere to explicitly simulate turbulent instabilities of the large-scale circulation.

Coupled Model Description

The global climate model used in this study is a prototype version of CCSM4; its components are the Community Atmospheric Model version 3.5 (CAM3.5), the Community Land Model version 3 (CLM3), the Los Alamos Parallel Ocean Program ocean general circulation model (GCM), version 2.0 (POP2) and the Community Ice Code version 4 (CICE4.0). CAM3.5 uses the Lin-Rood finite-volume dynamical core (Lin, 2004) and an updated CAM3 convection parameterization (Neale et al., 2008; Richter and Rasch; 2008). It was run on a 0.23° x 0.31° spherical grid with 26 levels. POP (Dukowicz and Smith, 1994) is configured on a 0.1°, 42-level tri-pole grid (Murray, 1996, Maltrud et al., 2010) with partial bottom cells (PBCs; Pacanowski and Gnanadesikan, 1998). The mixed layer parameterization in POP is the K-Profile Parameterization (Large et al., 1994). CICE 4.0 (LANL, 2008) uses the same horizontal grid as POP; CICE improvements are highlighted in Gent et al. (2009). The terrestrial component is the Community Land Model (CLM), version 3.0 (Dickinson et al., 2006).

CAM and CLM were started from rest. Initially the sea-ice was zonally symmetric with equatorward extents at 70°N and 60°S and with non-linear thickness distributions determined by latitude and SST. POP was initialized using a 2-year spun-up ocean state from an earlier CCSM simulation (same configuration except with a 0.5° atmosphere) in which POP was initialized at rest using potential temperature and salinity from the World Hydrographic Program Special Analysis Center (WHP SAC) climatology (Gouretski and Koltermann, 2004). Present-day conditions were represented by 1990's green house gas (GHG) forcing.

Climatology of the Coupled System

The coupled model used the standard set of atmospheric parameter (tuning) constants employed in the Gent et al. (2009) simulations. Significantly, the net energy imbalance at the top of the model was less than 1 Wm^{-2}. Similarly, the zonal distribution of net energy there was very close to values from Clouds and Earth's Radiant Energy System (CERES) observations, although the longwave and shortwave components had compensating zonal errors between 5 and 15 Wm^{-2} (in a mean of ~250-300 Wm^{-2}) in the mid-latitudes. Nevertheless, net heating is the dominant process that drives the climate system and determines the dynamic coupling between the atmosphere and ocean. A comparison of precipitation climatologies from CCSM4 and Xie-Arkin observations reveal errors that exceed 5 mm day^{-1} across a long and narrow band in the tropical north Pacific. Higher resolution does not improve the common problem of a double or split inter-tropical convergence zone (ITCZ). Other major errors are a precipitation deficit over the maritime continent and excess along the mountain ranges on the western coasts of the Americas. Although the split ITCZ is a nearly universal problem in coupled GCMs at all resolutions, the other errors expose the requirement to adjust precipitation and cumulus parameterizations to properly reproduce the physics on the correct scales.

The difference between climatological annual mean potential temperature from the upper-most ocean level (5m) for model years 13-19 and 0.25° daily Reynolds et al. (2007) satellite-derived sea-surface temperature (SST) data averaged over 1982-2008 (Fig 1a) is seen in Fig.1b. Cold biases dominate globally with extreme values of 10° and 6°C, respectively (Fig. 1b) occurring in the subpolar North Atlantic and Pacific; in the subtropics they are up to 1°C. The highest warm

104 biases are due to poleward displacements of the Gulf Stream and Kuroshio Extension (KE); more
105 modest biases are found across much of the tropical North Pacific (< 1°C) and in the Southern
106 Ocean (up to 2°C). In upwelling zones along the west coasts of North and South America SST is
107 generally up to 2°C too cold. Off the west coast of Africa between 0°and 20°S surface waters are
108 up to 2°C too warm. Warm biases of greater than 7°C were reported in these upwelling zones in
109 the standard CCSM3 (Collins et al. 2006). Gent et al. (2009) attribute their reduced SST biases in
110 these regions to better-resolved orography that situates stronger winds closer to the coast,
111 inducing increased upwelling.
112
113 Insight into some of the causes of the large-scale SST biases in the high and mid-latitudes are
114 obtained by examining the atmospheric circulation. In Fig. 2a and c we show annual
115 climatologies of 500 mb geopotential height and sea level pressure from European Center for
116 Medium-Range Forecasts-European Reanalysis 40 (ECMWF-ERA40), and in Fig. 3a surface
117 wind stress from QuikSCAT, together with the differences from CCSM4, averaged over model
118 years 13-19 (Figs 2b, d, and 3b). A major feature of this simulation is the intensification and
119 contraction of both polar vortices through the depth of the troposphere, which is likely related to
120 the strong numerical filtering required at high latitudes to keep the simulation computationally
121 stable at such fine resolution. In Fig. 2b, the geopotential height anomalies are less than -100 m
122 over Eurasia, while positive anomalies greater than 40 m can be seen over large areas between
123 40° and 60°S. The sea level pressure difference field (Fig. 2d) depicts the surface manifestation
124 of this problem, with excessively deep low-pressure systems over the poles and intensification of
125 the subtropical highs. The circulation around the intensified Azores High likely contributes to the
126 anomalously cold SSTs in the tropical Atlantic. Similarly the CCSM4-QuikSCAT wind stress

magnitude and vector differences show that CCSM4 winds are too strong over the subpolar North Pacific and North Atlantic oceans and over much of the Southern Ocean (Fig. 3b). Particularly, CCSM4 wind stress magnitudes exceed the QuikSCAT values by up to 0.09 Nm^{-2} in the eastern subpolar North Atlantic where the winds are south to southwesterly.

The Northern Hemisphere winter ice pack extends eastward across the entire Labrador Sea and reaches across the East Greenland Sea into the Norwegian Sea (not shown), implicating the overly intense polar atmospheric circulation in its setup. The North Atlantic Current fails to properly form the Northwest Corner and flows too far eastward across the North Atlantic. The too extensive ice pack results in anomalously cold surface waters located too far to the east in the North Atlantic subpolar gyre. Evaporative cooling of the surface water accompanies the overly strong subpolar winds that produce too strong Ekman currents that advect these cold surface waters toward the southeast, some of which enter the equatorward eastern boundary current. Subsequently this water circulates around the subtropical gyre contributing to the cold bias seen in Fig. 1b. This same process is active in the subpolar North Pacific.

Tropical Cyclone Event

A very positive feature of the simulation is its ability to generate and propagate intense, tropical cyclones when environmental conditions favor their development. To identify events in model years 13 through 19, we created animations of the 850 mb relative vorticity field (ζ_{850}), which was calculated from the 850 mb winds interpolated to a spectral resolution T63 grid (Bengtsson, et al. 2006). Possible cyclone events were associated with persistent vorticity centers exceeding 5

150 x 10^{-5} s^{-1}. More detailed analyses of individual storm events was performed using the full high
151 resolution output.
152
153 Compared to climatology, few storms were generated in the tropical North Atlantic, due to the
154 anomalously low SSTs (Fig. 1b) and accentuated Azores High (Fig. 2b). The animation of ζ_{850}
155 shows easterly waves forming off Africa, however no hurricanes developed in the tropical
156 Atlantic. A few waves that survived upon reaching the Gulf of Mexico did develop into storms
157 as a result of the more favorable local conditions. Conversely, the high SSTs in the tropical
158 northeastern Pacific permitted too many tropical storms to form (Fig.1b). Nevertheless, the high
159 resolution of the simulation permits the spontaneous generation and recurvature of Category 4
160 typhoons, as seen in an event with sustained 850 mb wind speeds of 66.5 ms^{-1} from July-August
161 of model year 19 over the western tropical Pacific.
162
163 The SST response under and to the right of the track is seen in Fig. 4a. The cold SST "wake" is
164 produced by the entrainment of cold subsurface water either through Ekman pumping or by
165 instability of the vertical shear of forced near-inertial oscillations. A surface temperature drop of
166 more than 3.6°C is seen at station 9 (133°E, 26°N) on 08/04/19, a day after the passage of the
167 storm over this location, relative to the pre-storm conditions on 07/29/19 (Fig. 4b). The ocean
168 mixed layer deepened from about 40 m to 80 m, while the temperature below the bottom of the
169 mixed layer and above 150 m increased by up to 2°C. Surface salinities increased from about
170 34.6 to 34.73 (not shown). By 08/18/19 the near-inertial oscillations had largely abated (not
171 shown), and the mixed layer shallowed to almost pre-storm conditions and warmed by 0.8°C.
172

The amount of net surface heating, Q, needed to restore the upper water column to pre-storm temperatures can be approximated by:

$$Q = \iiint \rho_0 C_P \Delta T dh dW dL = 5.8 \times 10^{20} J$$

where ΔT is the magnitude of the negative part of the temperature anomaly, h is the depth to which the negative part of the temperature anomaly extends, and dW and dL are the cross-track and along-track extents, respectively (Emanuel, 2001). The cross-track extent was identified by differencing SST before the storm and 24 hours afterwards; h was calculated using a 0.2° C threshold value of temperature from the 10 m value 24 hours after the storm's passage. Emanuel (2001) obtained a similar value of Q using approximate values for one North Atlantic hurricane event.

Ocean Mesoscale: Agulhas Eddy Pathways.

Agulhas leakage contributes some two-thirds of the upper limb of the Atlantic meridional overturning circulation (MOC) (Weijer et al., 1999). We compared Agulhas eddy tracks from satellite altimeter-derived sea surface height anomaly from AVISO for 2004-2008 and from CCSM4 for model years 15-19 (Fig. 6). We identified and tracked eddies using the Okubo-Weiss parameter, W, which measures the relative importance of deformation and rotation (Isern-Fontanet et al., 2003; 2006). Eddies were identified by closed contours of $W = -0.8 \times 10^{-12} s^{-2}$. AVISO shows three repeating (41, 42%, and 17%) northwesterly-directed pathways located progressively equatorward of each other by 2.5°of latitude; they terminate progressively eastward of each other at 32°W and 24°S, 25°W and 26°S, and 18°W and 26°S. CCSM4 shows two repeating tracks (78% and 13%) directed toward the northwest about 4° apart; they terminate

196 at 23°W, 25°S and 25°W, 21°S. Some latitudinal spread is seen in the cluster of pathways
197 constituting the primary pathway. Their signature disappeared slightly to the east of the observed
198 dissipation locations.
199
200 The CCSM4 Agulhas eddy pathways are more realistic than those in two earlier global stand-
201 alone 0.1° POP simulations, without (Maltrud and McClean, 2005) and with PBCs (Maltrud et
202 al., 2010), where the pathways angled too much toward the northwest and extended across the
203 entire South Atlantic. The path improvement may be due to compensating errors arising from the
204 positioning of the intensified subtropical gyre caused by the polar atmospheric circulation biases.
205 However the role of air-sea interactions cannot be ruled out in with regard to the eddy dissipation
206 locations, hence a follow-on study will examine feedbacks between local wind stress curl and
207 divergence, SST, and air-sea heat fluxes over individual eddies to better understand their
208 importance.
209
210 **Conclusions**
211
212 The simulation's climate is very reasonable considering that no tuning has been done to correct
213 for finer model resolution. It demonstrates the computational feasibility and model readiness to
214 execute coupled high resolution simulations and highlights the future potential of very high
215 resolution, long coupled climate runs to examine such features as decadal variability or the
216 contribution of ocean mixing in tropical storms to ocean heat transport. More importantly, the
217 simulation shows the potential for the spontaneous simulation of important coupled mesoscale

features that were previously impractical in a global coupled model, particularly the generation of intense tropical cyclones under the correct environmental conditions.

On the other hand, high-resolution does little to correct the large scale biases in the radiation and precipitation fields that most likely result from subgrid scale parameterization weaknesses. Furthermore, the high-resolution grid exacerbated well-known problems of finite-volume numerical methods on spherical coordinate grid systems, which likely resulted in the intensified and contracted polar vortices. The anomalous high latitude atmospheric circulation was reflected in surface wind stresses that were too strong in the subpolar North Atlantic, North Pacific, and the Southern Ocean. As a result, cold SST biases and excessive ice were created in the subpolar Northern Hemisphere. These anomalously low SSTs cause a dearth of hurricanes in the North Atlantic, while too high SSTs in the tropical eastern Pacific result in an excessive number of tropical systems forming in the North Pacific. Ongoing improvements in both the atmospheric dynamical core and atmospheric physics parameterizations will likely correct these shortcomings.

Acknowledgements

This work was supported by the Office of Science (BER), U.S. Department of Energy under contracts DE-AC52-07NA27344 (AAM, DCB, DPI, JSB, JLM), DE-AC05-00OR22725 (PHW, DCB), DE-AC02-06CH11357 (RLJ), DE-FG02-05ER64119 (JLM, YYK) and DE-AC52-06NA25396 (PWJ, MEM), and is released as LLNL Report LLNL-JRNL-XXXXXX. Accordingly, the U.S. Government retains a nonexclusive, royalty free license to publish or

reproduce the published form of this contribution, or allow others to do so, for U.S. Government purposes. Computer time was provided under LLNL's Multiprogrammatic & Institutional Computing Initiative. Altimeter products are from Ssalto/Duacs, Aviso and Cnes, ERA-40 reanalysis came from ECMWF and NCAR, and QuikSCAT winds are from JPL.

References

Bengtsson, L., K. I. Hodges, and E. Roeckner, 2006: Storm tracks and climate change, *J. Climate*, **19**, 3518-3543.

Dickinson, R.E., K.W. Oleson, G. Bonan, F. Hoffman, P. Thornton, M. Vertenstein, Z-L. Yang, and X. Zeng, 2006: The Community Land Model and its climate statistics as a component of the Community Climate System Model. *J. Climate*, **19**, 2302-2324.

Dukowicz, J. K. and R. D. Smith, 1994: Implicit free-surface method for the Bryan-Cox-Semtner ocean mode. *J. Geophys. Res.*, **99**, 7991-8014.

Emanuel, K., 2001: Contribution of tropical cyclones to meridional heat transport by the oceans, *J. Geophys. Res.,* **106**, 14771-14781.

Gent, P. R., S. G. Yeager, R. B. Neale, S. Levis, and D. A. Bailey, 2009: Improvements in a half-degree atmosphere/land version of the CCSM, *Clim. Dyn*., doi:10.1007/s00382-009-0614-8: Published online.

Gouretski, V. V. and K.P. Koltermann, 2004: WOCE global hydrographic climatology. Tech. Rep. **35**, Bundesamtes für Seeschiffahrt und Hydrographie, Hamburg, Germany.

Hack, J. J., J. M. Caron, G. Danabasoglu, K. W. Oleson, C. Bitz, and J. E. Truesdale, 2006: CCSM-CAM3 climate simulation sensitivity to changes in horizontal resolution, *J. Climate*,

19, 2267–2289.

Isern-Fontanet, J., E. Garcia-Ladona, and J. Font, 2003: Identification of marine eddies from altimetric maps, *J. Atmos. Oceanic Technol.,* **20**, 772–778.

Isern-Fontanet, J., E. Garcia-Ladona, and J. Font, 2006: Vortices of the Mediterranean Sea: An altimetric perspective, *J. Phys. Oceanogr.,* **36**, 87–103.

Large, W. G., J. C. McWilliams, and S. C. Doney, 1994: Oceanic vertical mixing: a review and a model with nonlocal boundary layer parameterization. *Rev. Geophys.*, *32*, 363-403.

Large, W. G., and G. Danabasoglu (2006), Attribution and impacts of upper-ocean biases in CCSM3, *J. Climate*, **19**, 2325-2346.

Lin S. J., 2004: A "Vertically Lagrangian" finite-volume dynamical core for global models. *Mon. Wea. Rev*. **132**, 2293–2307.

Maltrud, M. E. and J. L. McClean, 2005: An eddy resolving global 1/10 degree ocean simulation. *Ocean Modell.*, **8**, 31-54.

Maltrud, M., F. Bryan and S. Peacock, 2010: Boundary impulse response functions in a century-long eddying global ocean simulation. Environmental Fluid Mechanics, 10(1-2), 275-295. doi:10.1007/s10652-009-9154-3

McClean, J. L., M. E. Maltrud, and F.O. Bryan, 2006: Measures of the fidelity of eddying ocean models, *Oceanography*, 19, 104-117.

Murray R. J., 1996: Explicit generation of orthogonal grids for ocean models. *J*. *Comp*. *Phys.*, **126**, 251-273.

Neale, R. B., J. H. Richter, and M. Jochum, 2008: The impact of convection on ENSO: from a delayed oscillator to a series of events. *J. Climate*, **21**, 5904-5924.

Pacanowski, R.C. and A. Gnanadesikan, 1998: Transient response in a z-level ocean model that

resolves topography with partial cells, *Mon. Wea. Rev*., **126**, 3248-3270.

Reynolds, R. W., T. M. Smith, L. Chunying, D. B. Chelton, K. S. Casey, and M. G. Schlax, 2007: Daily high-resolution-blended analyses for sea surface temperature, *J. Climate,* **20**, 5473-5496.

Richter J H., and P. J. Rasch, 2008: Effects of convective momentum transport on the atmospheric circulation in the Community Atmosphere Model, version 3. *J*. *Climate*, **21**, 1487–1499. doi:10.1175/2007JCLI1789.1

Weijer, W., W. P. M. de Ruijter, H. A. Dijkstra, and P. J. van Leeuwen, 1999: Impact of interbasin exchange on the Atlantic overturning circulation, *J. Phys. Oceanogr*., **29**, 2266–2284.

Figure Captions

Figure 1. (a) Climatology of daily 0.25° Reynolds et al. (2007) satellite-derived SST (°C) data averaged for 1982-2008. (b) Difference field (°C) between the mean potential temperature for model years 13-19 from the upper-most model level (5m) and the observed SST climatology. Contour line is 0°C.

Figure 2. (a) Annual average of geopotential height at 500 mb from ERA40 and the (b) difference (m) of the model annual average geopotential height at 500 mb (m) and the ERA40 field. (c) Annual average of sea level pressure (mb) from ERA40 and the (d) difference (mb) of the model annual average sea level pressure and the ERA40 field.

Figure 3. (a) Annual average of wind stress magnitude (color contours) and vectors (Nm^{-2}) from QuikSCAT and (b) the difference of the model annual surface wind stress and the QuikSCAT field.

Figure 4. (a) Track of a Category 4 tropical cyclone event in July-August of model year 19 superimposed on the SST (°C) cold water "wake" under and to the right of the track of the center of the storm in the tropical northwest Pacific. (b) Vertical profiles of temperature (°C) at station 9 (133°E, 26°N) that correspond to pre-storm conditions (07/29/19), a day after the passage of the storm's center (08/04/19), and the water column once the near-inertial oscillations have largely abated (08/18/19).

Figure 5. Agulhas eddy pathways from (a) AVISO altimetry and (b) CCSM4. Numbers are percentage of times that eddies follow the same track.

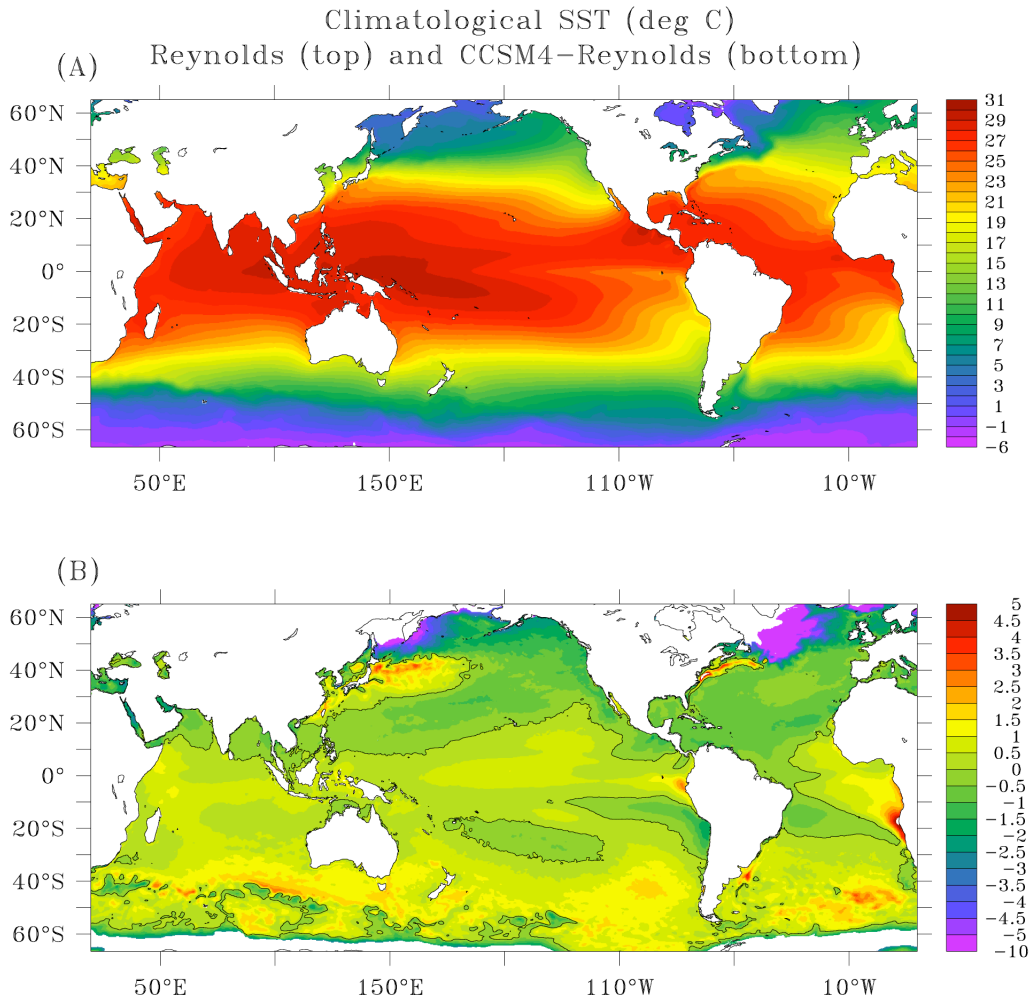

Figure 1: (a) Climatology of daily 0.25° Reynolds et al. (2007) satellite-derived SST (°C) data averaged for 1982-2008. (b) Difference field (°C) between the mean potential temperature for model years 13-19 from the upper-most model level (5m) and the observed SST climatology. Contour line is 0°C.

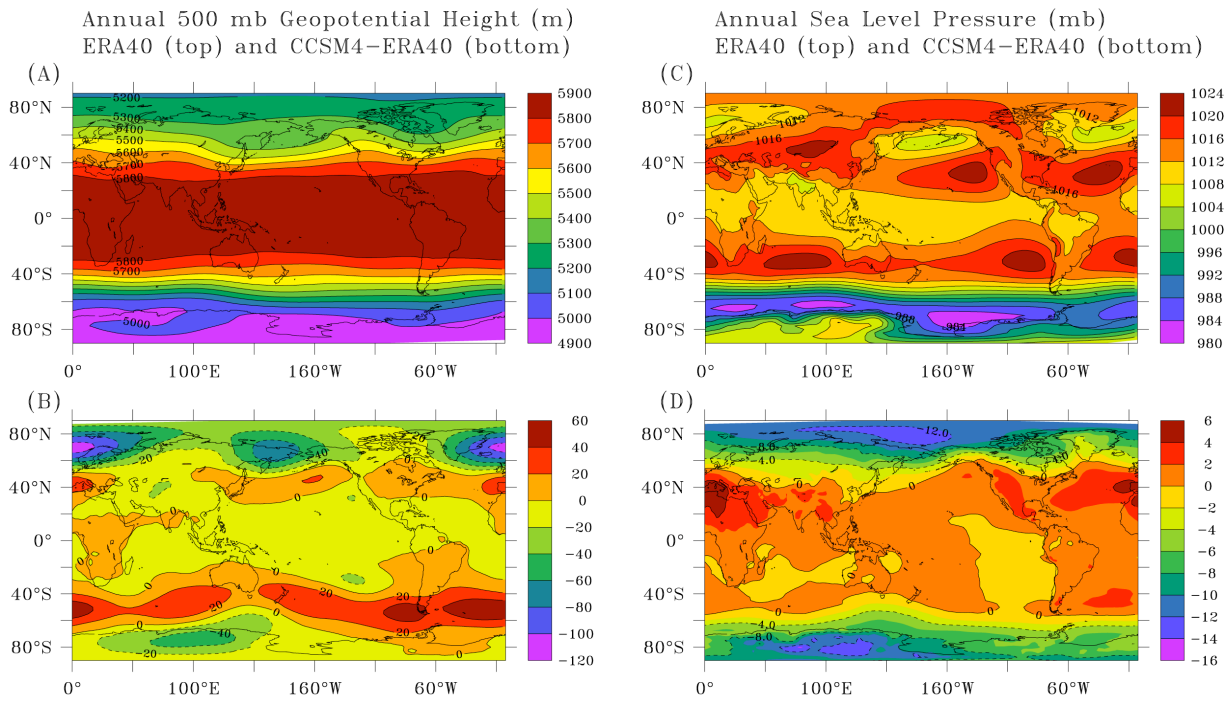

330

331 **Figure 2 (a): Annual average of geopotential height at 500 mb from ERA40 and the (b)**

332 **difference (m) of the model annual average geopotential height at 500 mb and the ERA40**

333 **field. (c) Annual average of sea level pressure (mb) from ERA40 (top) and the (d)**

334 **difference (mb) of the model annual average sea level pressure and the ERA40 field.**

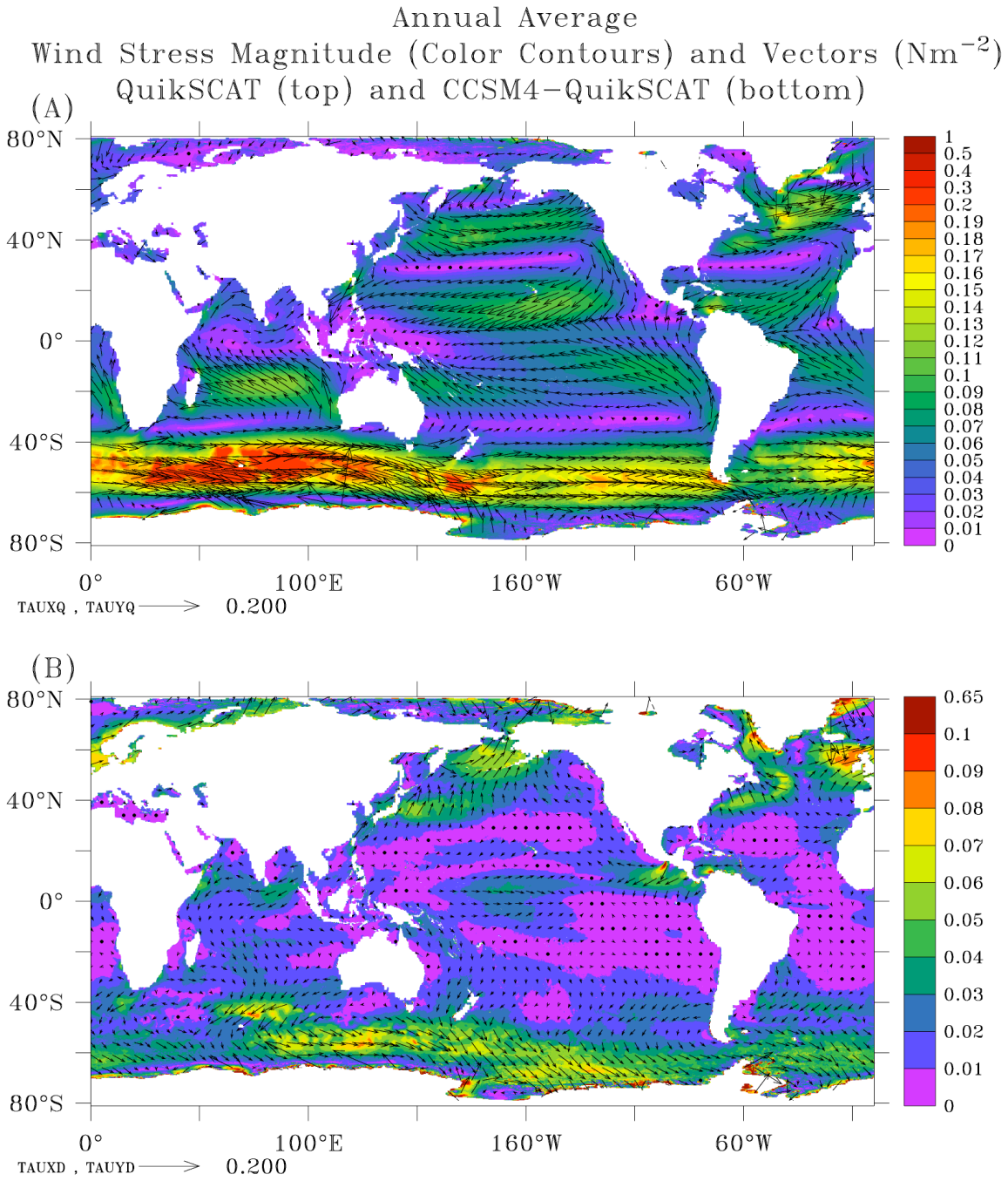

335

336 **Figure 3: (a) Annual average of wind stress magnitude (color contours) and vectors (Nm^{-2})**

337 **from QuikSCAT and (b) the difference of the model annual surface wind stress and the**

338 **QuikSCAT field.**

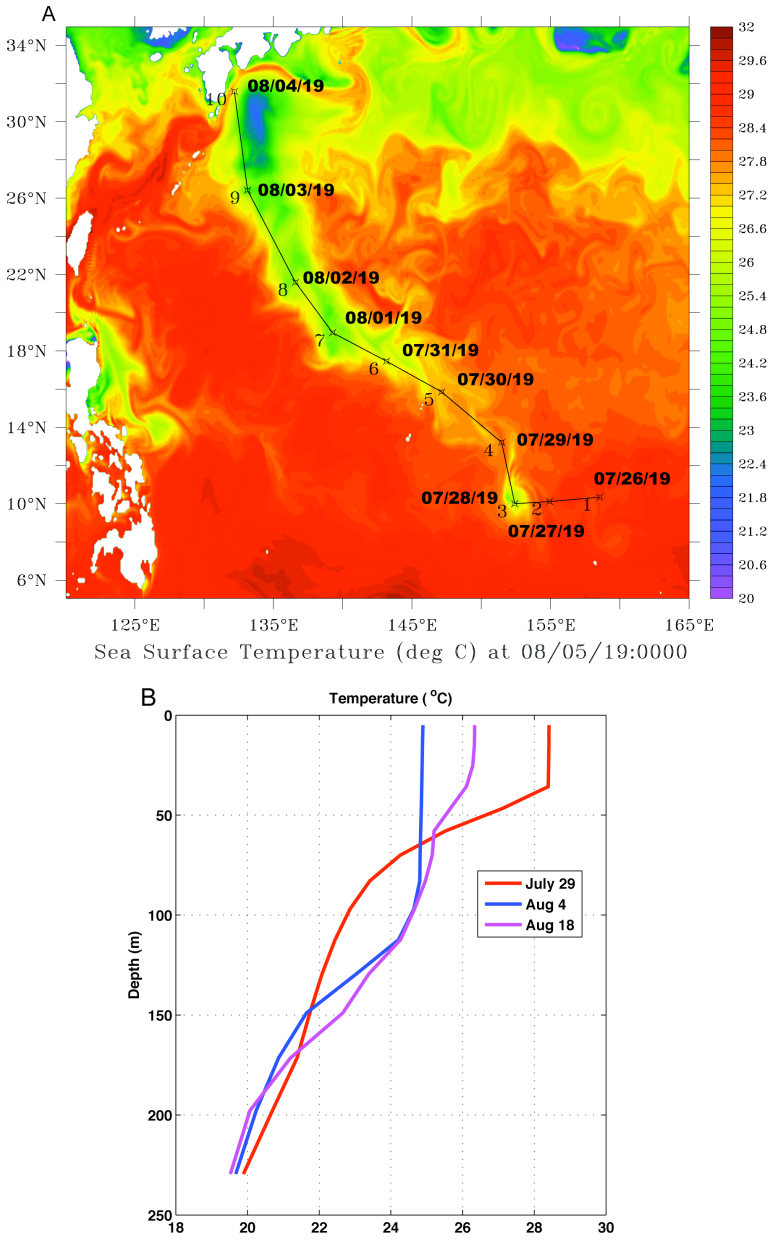

Figure 4: (a) Track of a Category 4 tropical cyclone event in July-August of model year 19 superimposed on the SST (°C) cold water "wake" on 08/05/19 in the tropical northwest Pacific. (b) Vertical profiles of temperature (°C) at station 9 (133°E, 26°N) that correspond to pre-storm conditions (07/29/19), a day after the passage of the storm's center (08/04/19), and the water column once the near-inertial oscillations have largely abated (08/18/19).

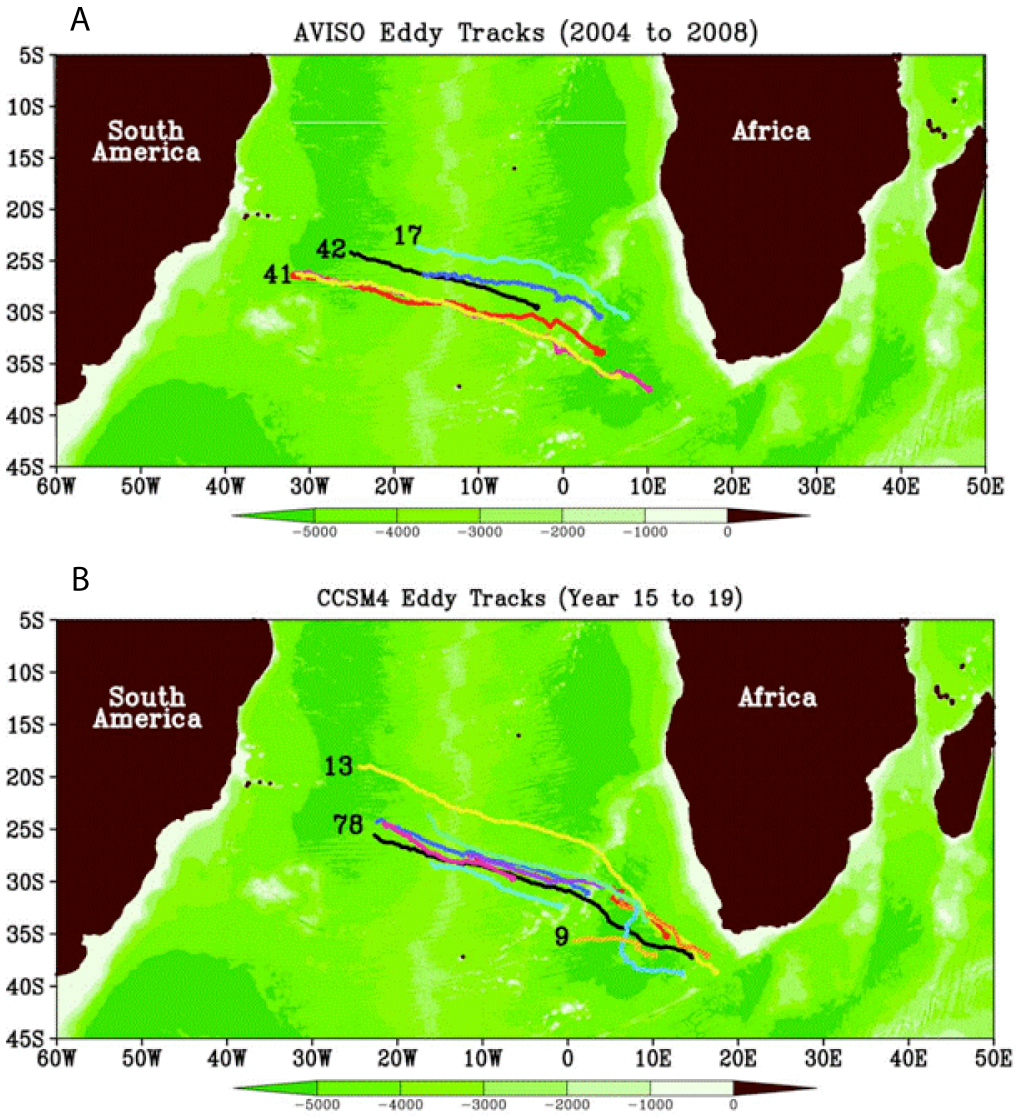

346

347 **Figure 5: Agulhas eddy pathways from (a) AVISO altimetry and (b) CCSM4. Numbers are**

348 **percentage of times that eddies follow the same track.**